Journal of Non-Crystalline Solids 546 (2020) 120268

Contents lists available at ScienceDirect

Journal of Non-Crystalline Solids

journal homepage: www.elsevier.com/locate/jnoncrysol

Comparison of structural, physical and optical properties of Na_2O-B_2O_3 and Li_2O-B_2O_3 glasses to find an advantageous host for CeO_2 based optical and photonic applications

Gurinder Pal Singh[a,*], Joga Singh[a], Parvinder Kaur[a], Simranpreet Kaur[b], Deepawali Arora[b], Ravneet Kaur[c], D.P. Singh[b]

[a] P.G. Department of Physics, Khalsa College, Amritsar 143002, India
[b] Department of Physics, Guru Nanak Dev University, Amritsar 143005, India
[c] P.G.Department of Physics, Lyallpur Khalsa College, Jalandhar 144001, India

ARTICLE INFO

Keywords:
Glasses
Cerium
Elastic constant
Lithium;s sodium

ABSTRACT

This study focuses on alkali oxide (lithium and sodium) glasses with an aim to explore suitable host for cerium ions which will enhance the optical properties like UV blocking efficiency. Conventional melt quench method was employed for making these glasses. FTIR results show conversion of BO_3 to BO_4 units and development of CeO_4 groups with addition of CeO_2. The increase in density values (2.10 to 2.67 g/cm^3 for sodium glasses and 2.04 to 2.75 g/cm^3 for Lithium glasses) and decrease in band gap values (3.16 to 2.40 eV for sodium glasses and 3.28 to 2.08 eV for Lithium glasses) in both glass systems confirm the modifier role of CeO_2. Hardness of lithium-based glasses (1366.91 Kg/mm^2) at 4 mol% of CeO_2 is higher than the glasses containing sodium (1007.21 Kg/mm^2). The obtained values of refractive index and transmittance show better suitability of CeO_2 incorporated lithium glasses in some optical applications.

1. Introduction

Glass is the most frequently used material these days ranging from domestic goods to advance technologies. Topical progression in the glass field facilitates the researcher to design numerous kinds of oxide glasses such as phosphate, borate, germanate, silicate, tellurite etc. But due to the various uses of borate glasses, these glasses are more important as compared to other oxide glasses. Borate glasses are fascinating due to their advantageous properties like chemical durability, low melting temperature, high transparency, good alkali/transition/rare-earth ions solubility and good thermal stability [1-3]. These glasses are one of the best glass formers but an incorporation of any network modifier (like alkali/TMO/RE) to borate glass system helps to break the B-O bonds and encourages the change of triangular BO_3 units to tetrahedral BO_4 units [4-7]. In alkali metals, sodium or lithium-based borate glasses are the most resourceful glass systems [8-12]. Lithium added glasses have many advantageous properties like strength, polaron character and wide range formability. For these reasons, they are used as dosimeter fabrication materials [13], radiation shielding materials [14], energy storage electrode materials [15-16] and in optoelectronic devices applications [17], optical fiber communication [18], dental applications [19], lithium-ion conducting glasses [20] and photonic applications [21].

High sodium binary borate glasses have their local structure qualitatively similar to lithium borate glasses of similar composition as indicated by earlier investigations [22]. The role of the sodium borate glasses as a modifier is used in different techniques. [23-25]. Sodium addition in glasses system helps to modify the stability, hinder the moisture and turn down the temperature process [26]. Due of their simple fabrication and flexibility to insert active ions in different concentrations like TMO/RE ions, Sodium oxide glasses are studied as good host materials [27-29]. The sodium glasses have garnered wide consideration in the past many years due of their technical, innovative and industrial benefits in applications such as enamels, photonics and optoelectronics [30]. With the addition of various transition metal ions like TiO_2, Fe_2O_3, Cr_2O_3, CuO, ZnO, NiO and $MnCO_3$, luminance behaviors of sodium glasses are investigated by Hongli Wen [31]. The additions of rare earth ions in sodium glasses are prospective candidates for many good applications in optics, for example, they are used to prepare laser with reddish-orange emission [32]. These glasses are used in storage applications [33] and also as shielding materials for gamma rays [34-35]. Recently some research groups find tremendous applications of

* Correspondence author: Gurinder Pal Singh P.G. Department of Physics, Khalsa College, Amritsar 143002, India.
E-mail address: gp_physics96@yahoo.co.in (G.P. Singh).

https://doi.org/10.1016/j.jnoncrysol.2020.120268
Received 10 May 2020; Received in revised form 23 June 2020; Accepted 24 June 2020

sodium glasses as radiation dosimeters [36], to make coloured LEDs [37] and used to develop an efficient method for extracting palladium from spent automobile catalyst [38].

Besides, these glasses are dexterous host systems to include a high content of rare earth metal oxides, for example cerium oxide [39-41]. The cerium ions have enormous importance that comes from their fascinating uniqueness such as physical, catalytic and optical properties [42-46]. It plays the intermediating role depending upon its quantity in borate glasses.

Due to co-existence of Ce^{3+} and Ce^{4+} ions, cerium doped glasses are very important for their excellent lasing/optical properties and strong optical absorption in near UV or Visible region [47]. So these are used in a variety of technological applications such as scintillators, luminescent materials, detection of X-rays and solid-state lasers [48-53]. Cerium containing mesoporous glasses are used for bone regeneration [54] and also show Magneto-optical [55] and super-paramagnetic behaviour [56]. Recent studies have showed that cerium glasses can also be used as potential candidates as white light emitters i.e. white LEDs [57], radiation shielding [58] and Thermoluminescence materials [59].

In view of past studies on alkali borate glasses by different researchers, here we are trying to find new and proficient host-ion composition that will be capable of high stability and strong UV blocking tendency. In the present investigation, our main concern is a comparative study (structural, physical and optical) of two glass systems (sodium and lithium) with the incorporation of cerium oxide. In this way, the present study also tried to search excellent optical materials for future UV blocking and optical filters applications.

2. Experimental procedure

2.1. Sample preparation

The two systems of glasses 70 B_2O_3–(30-x) AO-xCeO_2 (where x = 0, 1, 2, 3 and 4 in the molar ratio and AO = Na_2O, Li_2O) are prepared by using Melt quench technique. The raw materials used are given in Table 1. The mixture was thoroughly ground and melted at 1070–1100 °C for 60 min in silica crucible until a bubble-free liquid is formed. The homogenized melt is then quenched in air by pouring it on to preheated steel mold and annealed at a temperature of 370 °C for one hour to avoid breaking of the sample by residual internal thermal strains. The obtained samples were polished with cerium oxide in order to obtain maximum flatness. The investigational methods are similar as mentioned in our earlier study [60].

The amorphous/crystalline nature of the samples was confirmed by X-ray diffraction (XRD) study using (Shimadzu, Japan) X-ray diffractometer at the scanning rate of 2°/min and 2θ varying from 10–70°

The density of glass samples at room temperature was measured by the standard principle of Archimedes using a sensitive microbalance with pure benzene as the immersion fluid. The formula for density is mentioned in Table 2.

Table 1
Nominal composition (mole fraction) of different components used.

Sample Code	CeO_2	Na_2O	Li_2O	B_2O_3
NaBC0	0	30	0	70
NaBC1	1	29	0	70
NaBC2	2	28	0	70
NaBC3	3	27	0	70
NaBC4	4	26	0	70
LBC0	0	0	30	70
LBC1	1	0	29	70
LBC2	2	0	28	70
LBC3	3	0	27	70
LBC4	4	0	26	70

Table 2
Equations of different structural, physical and optical parameters.

Parameter	Formula	References
Density (ρ)	$(\frac{W_A}{W_A - W_B}) \times \rho_b$	60–61
Molar Volume (V_m)	$\frac{M}{\rho}$	60–61
Average boron–boron separation	$\langle d_{B-B} \rangle = (\frac{V_m^B}{N_A})^{\frac{1}{3}}$	69–70
Molar volume of oxygen	$V_0 = \sum_i \frac{V_m}{x_i n_i}$	69–70
Oxygen Packing Density	$OPD = 1000C(\frac{\rho}{M})$	69–70
Refractive index	$(\frac{n^2-1}{n^2+2}) = (1 - (\frac{E_g}{20})^{1/2})$	69
Ion concentration (N)	$\frac{Density(\rho) \times AvogadroNo.(N_A) \times mole\%(RE)}{AveragaeMolecularweiight(M)}$	71–72
Polaron radius r_p(Å)	$\frac{1}{2}(\frac{\Pi}{6N})^{1/3}$	71–72
Inter nuclear distance r_i(Å)	$(\frac{1}{N})^{1/3}$	71–72
Field strength (F)	$\frac{Z}{r_p^2}$	71–72
Poisson ratio (σ)	$\sigma = (0.5) - (\frac{1}{7.2V_T})$	75
Packing Density (V_T)	$V_T = \sum \frac{V_i x_i}{V_m}$	75, 79, 81
Young's Modulus of Elasticity (E)	$E = 83.6 \sum G_i x_i$	79, 81
Modulus of Compressibility (K)	$K = \frac{E}{3(1-2\sigma)}$	79, 81
Modulus of Elasticity in Shear (G)	$G = \frac{E}{2(1+2\sigma)}$	79, 81
Electronegativity (χ)	$\chi = 0.2688\ E_g$	70, 75
Electronic Polarizability (α_e)	$-0.9^*\chi + 3.5$	70, 75
Theoretical Basicity (Λ_{Th})	$\Lambda_{Th} = -\chi^*0.5 + 1.7$	70, 75
TPA (cm/GW)	β (cm/GW) = [36.76 - 8.1 Eg]	69
Bond Density (n_b)	$n_b = \frac{N_A}{V_m} \sum_i n_c x_i$	69

The Optical Absorption spectra of polished samples were recorded at room temperature by using UV–Visible Spectrophotometer (Perkin Elmer) in the range 200–900 nm.

The infrared transmission spectra of the glasses were measured at room temperature in the wave number range 400–4000 cm^{-1} by a Fourier Transform computerized infrared spectrometer (Thermo Nicolet 380 spectrometer). The prepared glasses were mixed in the form of fine powder with KBr in the ratio 1:100. The weighed mixtures were then subjected to a pressure of 150 kg/cm^2 to produce homogeneous pellets. The infrared transmission measurements were taken immediately after preparing the pellets. The calculation of other different theoretical parameters is mentioned in Table 2.

3. Results and discussion

3.1. X-Ray diffraction (XRD) analysis

The XRD studies of all the 70 B_2O_3–(30-x) AO-xCeO_2 (where x = 0 to 4 the mole% and AO = Na_2O, Li_2O) glasses are depicted in Fig. 1. The occurrence of wide humps emerging in the spectra of these glasses is indicative of the fact that the prepared samples are amorphous in nature [61]. This correlates well with the experimental findings that the atoms are neither regularly spaced nor uniform in glasses contrary to crystals.

3.2. Infrared spectra

Infrared study is a potent tool to have an in-depth analysis of the glass framework in terms of the structural units, bridging bonds of oxygen and inhomogenities present in the structure. The IR vibrations of the present study are mainly active in the central infrared region i.e. 400–2000 cm^{-1} as exposed in the Fig. 2 and 3 and thereby can be separated into three sections:

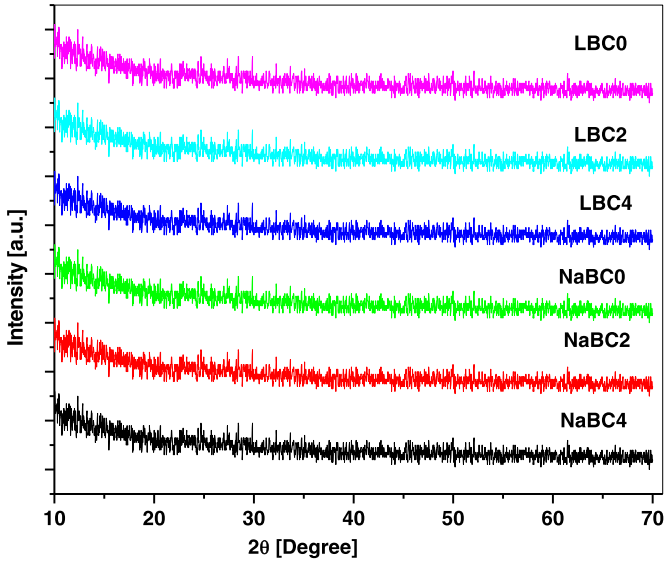

Fig. 1. X -Ray diffraction of sodium and lithium glasses.

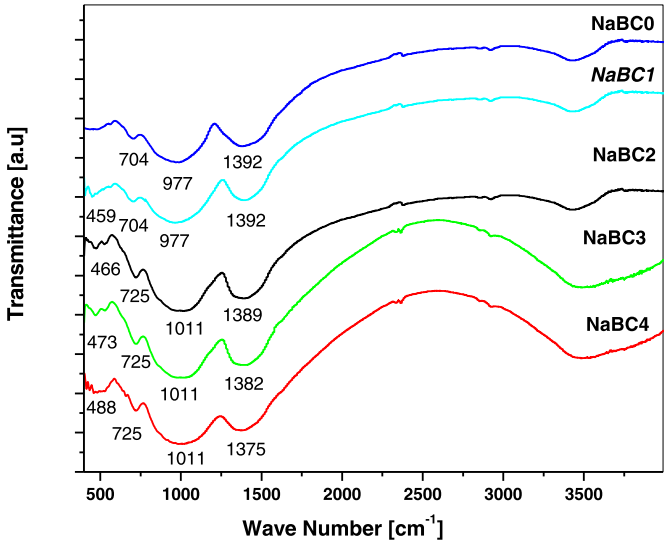

Fig. 2. FTIR Spectra of CeO_2—Na_2O-B_2O_3 glasses.

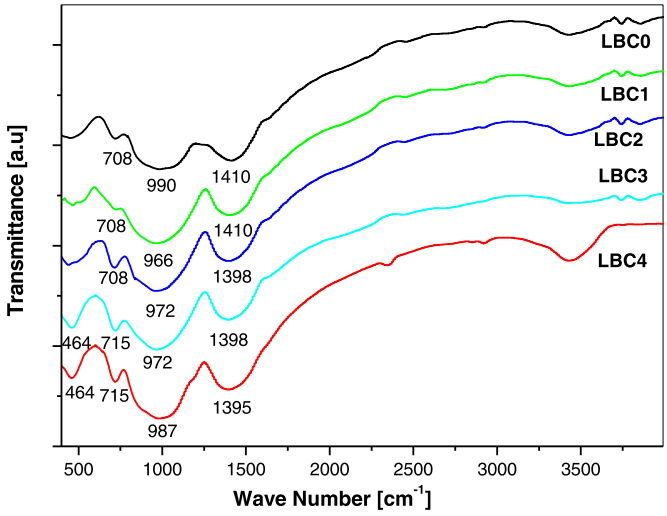

Fig. 3. FTIR Spectra of CeO_2-Li_2O- B_2O_3 glasses.

(i) in the section 600–800 cm^{-1}; (ii) in the section 800–1200 cm^{-1} and (iii) in the section 1200–1600 cm^{-1} [62-63].

3.2.1. *Infrared spectra of 70 B_2O_3–(30-x) Na_2O-xCeO_2*

The IR vibrations of the samples NaBC0, NaBC1, NaBC2, NaBC3 and NaBC4 are represented in Fig. 2. The IR band appearing in all the glass samples between 704727 cm^{-1} is B–O–B bending vibration of [BO_3] groups in the glass [64]. This band becomes even more prominent in the compositions NaBC1, NaBC2, NaBC3 and NaBC4 where there is an increase in the concentration of the Ce ions at the expanse of Na ions and shifts towards higher wavenumber side gradually. At an elevated value of cerium, a novel weak band emerges in these samples at 459–488 cm^{-1} which is not present in the base sample NaBC0. The manifestation of this feeble band can be allied to the vibrations of cerium ions linked in the glass matrix besides the stretching of B-O bonds [65]. This band is usually owing to the existence of stretching vibration of Ce–O bond in CeO_4 groups of cerium [65]. The shifting of this band with enhances in cerium quantity is an indication that the occurrence of cerium makes available surplus oxygen to network and facilitates the creation of such structural groups with boron. The IR band in the second region ranging from 800 cm^{-1} to 1200 cm^{-1} is prevalent at 977 cm^{-1}. This band is ascribed to the stretching vibrations of the B–O bonds in BO_4 units in tri-, tetra- and penta-borate groups [66]. There is a slight shifting of this band towards higher wavelength along with the increase in its intensity in the samples NaBC3 and NaBC4. This observation leads to the conclusion that with the increase in cerium content (0–2 mol), the BO_3 structural groups are transformed into tetrahedral BO_4 units indicating that cerium enters into the glass network as a modifier. In addition, a broadband located in the province ~1200–1600 cm^{-1} is observed at 1392 cm^{-1} which is associated with B-O stretching vibration of BO_3 units in various borate groups such as meta-, pyro- and ortho-borate groups [67]. The water groups are noticeable by the occurrence of bands above 2000 cm^{-1}.

3.2.2. *Infrared spectra of 70 B_2O_3–(30-x) Li_2O-xCeO_2*

The IR spectrum of the glasses containing Li ions is given in Fig. 3. The samples are labeled as LBC0, LBC1, LBC2, LBC3, and LBC4 as per the variation in their composition. In general, there are three broad intense bands that appear in all the samples, the first one between ~708–715 cm^{-1}, second at 966–990 cm^{-1} and the third one at ~1395–1410 cm^{-1}. These bands represent the characteristic features of borate glasses. There are main differences between the spectra of 70 B_2O_3–(30-x) Li_2O-xCeO_2 and 70 B_2O_3–(30-x) Na_2O-xCeO_2 glasses as summed up below. The first one is the increase in the intensity of the band among 400–500 cm^{-1} in the 70 B_2O_3–(30-x) Li_2O-xCeO_2 glasses. This band is indicative of the Ce-O bonding which begins in the borate network in Na1, Na2, Na3 and Na4 glasses [65]. The increase in intensity of this band in 70 B_2O_3–(30-x) Li_2O-xCeO_2 glasses indicates that although the addition of Ce ions to the lithium borate network causes the development of cerium units (CeO_4) shared with the borate network yet this effect is more pronounced as compared to Na ions. Further, it can be assumed that the lithium glass series has a higher concentration of symmetric BO_4 groups as compared to sodium glass series. This seems to be further true for the region 800–1200 cm^{-1}. In Li based glasses, the bands appearing in the region 966–990 cm^{-1} are due to di- and tetra- borate groups [66-67], however in Na based glasses the bands are seen in between 9771011 cm^{-1} due to tetra-, penta-borate groups of BO_4 [66-67]. Analogous trend is observed in the third region i.e. 1200–1600 cm^{-1}, where the Li based glasses show IR vibrational modes located from 1395 to 1410 cm^{-1} [66-67]. This region is characteristic of BO_3 units and it is shifting towards lower frequencies. Here, one thing that is observed in LBC glasses as compared to NaBC glasses is that the intensity of the band between 8001200 cm^{-1} increases and the intensity of region 1200–1400 decreases due to addition of cerium. This shows that in Li glasses, BO_4 units are dominant rather than tetrahedral BO_3 units [60].

Table 3
Physical Parameters.

Sample Code	NaBC0	NaBC1	NaBC2	NaBC3	NaBC4	LBC0	LBC1	LBC2	LBC3	LBC4
Density (D) (g/cm^3)	2.1	2.23	2.35	2.48	2.67	2.04	2.16	2.29	2.53	2.75
Molar Vol. (cm^3/mol)	32.06	30.69	29.59	28.48	26.87	28.29	27.38	26.44	24.5	23.05
$<d_{bb}>$ (nm)	0.446	0.44	0.434	0.429	0.42	0.428	0.423	0.418	0.408	0.4
V_0	13.36	12.73	12.23	11.72	11.01	11.79	11.36	10.93	10.09	9.45
OPD	74.85	78.53	81.78	85.31	90.81	84.84	88.03	91.52	99.2	105.84
Bond density (n_b)	0.751	0.789	0.822	0.859	0.915	0.852	0.884	0.92	0.998	1.066
Average Molecular weight (M)	67.34	68.44	69.54	70.64	71.74	57.71	59.13	60.56	61.98	63.4
Number density: N (*10^{20} ions/cm^3)	0	1.96261	4.07092	6.3437	8.96648	0	2.20007	4.5554	7.376	10.45007
Polaron radius (r_p) (Å)	0	1.494	1.171	1.01	0.9	0	1.438	1.128	0.961	0.855
Inter-nuclear distance (r_i) (Å)	0	3.707	2.907	2.507	2.234	0	3.569	2.8	2.385	2.123
Field Strength (F) (*10^{17}cm^{-2})	0	2.599	4.23	5.686	7.161	0	2.805	4.558	6.28	7.934
Number density: N (*10^{20} ions/cm^3)	0	1.96261	4.07092	6.3437	8.96648	0	2.20007	4.5554	7.376	10.4501
Polaron radius (r_p) (Å)	0	1.494	1.171	1.01	0.9	0	1.438	1.128	0.961	0.855
Inter-nuclear distance (r_i) (Å)	0	3.707	2.907	2.507	2.234	0	3.569	2.8	2.385	2.123
Field Strength (F) (*10^{17}cm^{-2})	0	2.599	4.23	5.686	7.161	0	2.805	4.558	6.28	7.934

In lithium glass series, intensity of the band located between 700800 cm^{-1} decreases firstly with the incorporation of cerium oxide but with the increment in the quantity of cerium, the intensity of this band increases further and it shifts from 687 to 693 cm^{-1}. It may be due to creation of a new kind of bonds (B-O-Ce) by demolishing B-O-B linkages in the borate matrix [67-68].

3.3. Density and molar volume

The density of glass is an imperative consideration for industrialized/commercial fabrication of glass and is fundamental for calculating other parameters such as refractive index, molar volume, elastic properties and even thermal conductivity. The calculated values of density, molar volume, and boron-boron separation of the NaBC and LCB glass systems are given in Table 3, along with various further physical parameters. In sodium glasses, the density gets augmented from 2.10 to 2.67 gm/cm^3 due to the increase in the quantity of cerium oxide. Alike behavior is shown for LBC glass systems where it is seen that the density gets enhanced from 2.04 to 2.75 gm/cm^3. It is evident that the inclusion of modifier oxides like, cerium oxide into glass network is mindful of the change of BO_3 components into more compact tetrahedral [BO_4] components [60-61]. But the gradual increase in density of NaBC and LBC glass systems can be also be attributed to the fact that a bigger, heavier and denser CeO_2 replaces Li_2O as well Na_2O molecules in the random glass framework. The decrease in molar volumes for both the series with an increase in cerium content further correlates with the density measurement that higher atomic mass of cerium ions increases oxygen packing density thereby making the structure more compact [61].

The outcomes appeared in Table 3 demonstrated that a constant diminish in the average boron–boron separation $\langle d_{b\text{-}b} \rangle$ with the addition of cerium oxide and the glass arrangement appears a diminishing proclivity for extension [69-70]. But this impact is more articulated in glasses containing lithium oxide. It once more affirms the compact structure or densification of both glass frameworks.

Density and molar volume results are well upheld by V_0 and OPD values (Table 3). These are in an inverse relationship (V_0 diminishes and OPD rises) [70]. This behavior unveils the non appearance of non-bridging oxygen and arrangement of bridging oxygen with the consolidation of CeO_2 in glasses. These bridging oxygens construct the glass structure firmly packed.

The average rare-earth ion concentrations (N), polaron radius (r_p), inter-nuclear distance (r_i) and field strength (F) of Ce–O bond of cerium have also been found out using standard formulae given in Table 3 [71-72].

This perception was ascribed to the overfilling of cerium ions inside the glass matrix. This in turn obviously improved the field strength [71-72]. These parameters are being more influenced in the lithium borate glass system with the quantity of CeO_2. Hence it discloses that lithium borate glass system is more suitable for cerium ions.

The addition of cerium contents in both the glass series helps to reduce the polaron radius as well as inter-nuclear separation. Table 3 shows that the polaron radius (r_p) is 2.5 times smaller in comparison with the inter-ionic distance (r_i) and hence these smaller (r_p) values have resulted in a higher field strength (F) [73]. From Fig. 4, it can be found that with increase in Ce concentration, interionic distance decreases which might be due to enhanced compactness and decrease in the distance between rare earth ion and oxygen. As a result of this, the bond strength between rare earth ion and oxygen increases, producing more field strengths around the rare earth ion concentration [71-72]. The optical basicity values for the present glasses are increasing with increase in the concentration of Ce ions specifying the increase in the negative charge on the oxygen atom.

Comparing the values of the optical basicity as given in table 4, we can say that cerium glasses containing lithium would be more useful as compared to sodium glasses for designing the novel optical functional materials with higher optical performance. Also the refractive index of lithium glass matrix is on higher side. These parameters are being more influenced in the lithium borate glass system with the quantity of CeO_2. Hence it discloses that lithium borate glass system is more suitable for cerium ions.

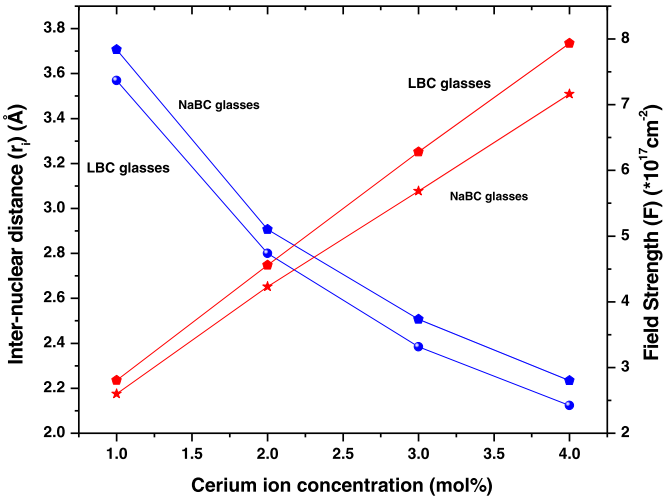

Fig. 4. Variation of inter-nuclear distance and field strength with cerium ion concentration.

Table 4
Optical Parameters.

Sample Code	NaBC0	NaBC1	NaBC2	NaBC3	NaBC4	LBC0	LBC1	LBC2	LBC3	LBC4
Optical Band Gap ($E_{opt.}$) (eV)	3.16	2.82	2.63	2.5	2.4	3.28	2.7	2.56	2.31	2.70
Refractive index	2.36	2.45	2.51	2.55	2.58	2.33	2.48	2.53	2.61	2.70
Electronic polarizability ($Å^3$)	2.736	2.818	2.864	2.895	2.919	2.707	2.847	2.881	2.941	2.997
Theoretical Optical basicity	1.2753	1.32099	1.34653	1.364	1.37744	1.25917	1.33712	1.35594	1.38954	1.42045
TPA	11.164	13.918	15.457	16.51	17.32	10.192	14.89	16.024	18.049	19.912

3.4. Refractive index and electronic polarizability of glasses

The refractive index value of both glass series enhances regularly with a shrink in the optical band gap corresponding to an increase in CeO_2 quantity [69]. The subsequent reasons are accountable for augmentation in refractive index;

(a) The refractive index of glasses is directly dependent on the density of respective glasses i.e. higher the value of density, higher will be the refractive index of glasses.
(b) The change in the coordination of borate from trigonal BO_3 to tetrahedral BO_4.
(c) The polarizability of Ce^{4+} (0.738 Å) has greater value as compared to Na^+ (0.181 $Å^3$), Li^+(0.029 $Å^3$) and B^{3+} (0.003 $Å^3$) [74].

3.5. Optical study

UV-Vis absorption spectrums of the two glass series are displayed in Fig. 5 and 6 which are used to inspect the UV-shielding capability of these glasses. Clearly in both the glass series, the absorption edge is shifting towards the longer wavelength i.e. red shift is observed. In LBC glasses, this shift (from 355–488 nm) is more pronounced as compared to sodium glass series (from 358- 452 nm).

As an optical band energy is a bond delicate property, so any change in the optical energy gap is directly related to any change in average bond energy. The optical energy gap is computed by means of a graph between $(\alpha h\nu)^{½}$ and energy ($h\nu$) as depicted in Fig. 7 for CeO_2–Na_2O-B_2O_3 and for CeO_2-Li_2O-B_2O_3 glasses in Fig. 8. The data represented in Table 4 interpreted that the energy value E_{opt}, of both the glass series has decreased with the inclusion of CeO_2. But this decrement is more effective for the lithium borate glasses (LBC) (from 3.28 to 2.08 eV) than Na_2O-B_2O_3 glasses (from 3.16 to 2.40 ev). This observation showed that the presence of cerium plays a more governing job in the LBC glass matrix. The shifting of absorption edge and corresponding shrinkage in the energy band gap of both glass series depends upon the various factors that are explained below

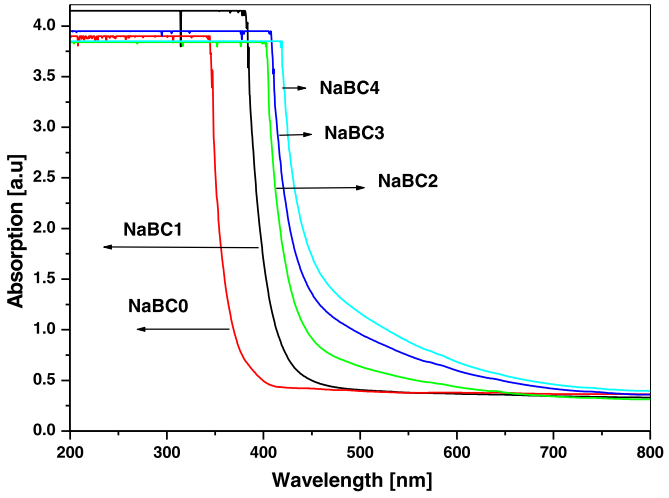

Fig. 5. Optical Absorption of CeO_2–Na_2O-B_2O_3glasses.

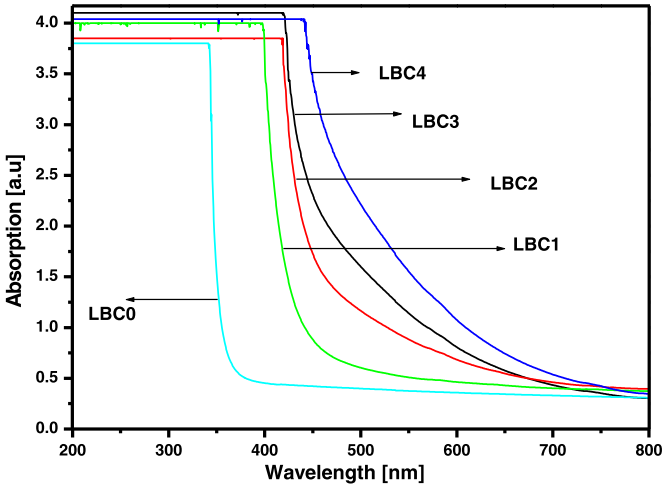

Fig. 6. Optical Absorption of CeO_2-Li_2O-B_2O_3glasses.

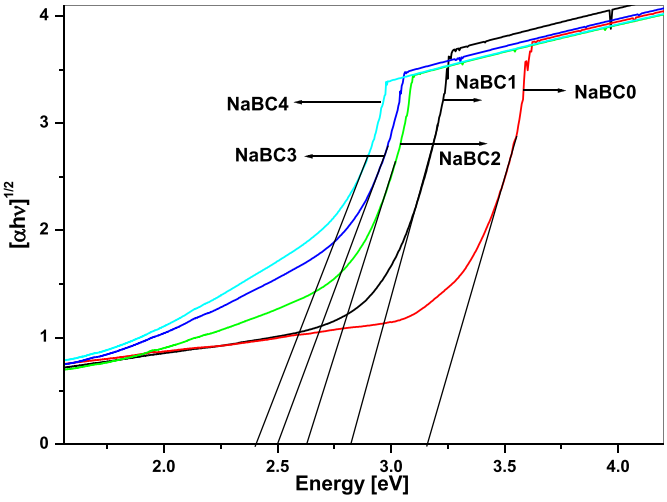

Fig. 7. Optical Band gap of CeO_2–Na_2O-B_2O_3glasses.

(a) CeO_2 inclusion in the glass template facilitates to alter the trigonal BO_3 to BO_4 units. These tetrahedral groups have the tendency to make a more strongly bonded glass system as compared to trigonal BO_3 groups. This is due to the fact that tetrahedral [BO_4] components of borate are much denser than [BO_3] groups; consequently, there is an improvement in the connectivity of the glasses network [60].
(b) One more reason for edge shift towards the higher wavelength side is the conversion of Ce^{3+} ions to Ce^{4+}ions. Here it is exposed that the addition of cerium oxide in lithium glasses makes more suitable environment that favours the construction of more Ce^{4+} ions [60-61].

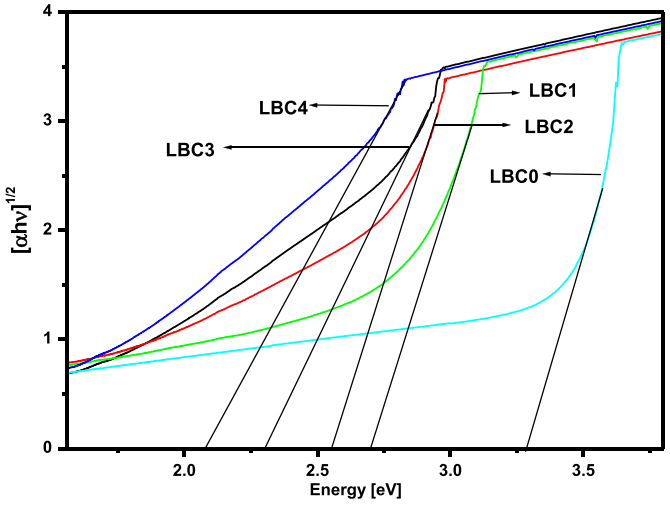

Fig. 8. Optical Band gap of CeO_2-Li_2O-B_2O_3glasses.

Outcomes of optical basicity (OB) and electronic polarizabilityas shown in Table 4 may also help to explain the contraction of energy gap and shifting of the absorption edge of glasses. Basically, optical basicity is the electron-donating ability of the oxygens in the glass scheme [57] and it is strongly affected by variation in electronic polarizability. Basicity has been proven to be a vital factor for calculating the properties of a glass system before applying the glass in diverse applications. The theoretical optical basicity can be determined based on the accompanying condition proposed by X. Zhao et al. [75]. The optical basicity value gets augmented significantly with the insertion of CeO_2 [Table 4]. Electronic polarizability is in the directly proportional relation with basicity [75]. The higher value of optical basicity means an enhanced ability of oxide ions to transfer negative charge electrons to the surrounding cations. A few of this electron density is situated among the inner electron core of the Ce^{3+} ion and its 4f orbital. This factor creates a screening effect between the force of attraction between the nucleus and 4f electron of Ce^{3+} ions which allows the 4f electron to escape easily. These factors are favouring that Ce^{3+} ions are converting to Ce^{4+} ions by losing a 4f electron [76].

$$Ce^{3+} \rightarrow Ce^{4+} + e^{-}$$

(a) Another factor that is responsible for the decreased band gap is the bond strength value between the cation and oxygen bond. The single covalent bond energy value of heteronuclear bond D(A-O) can be calculated by using the relation [69]

$$D(A-O) = [D(A-A)\times D(O-O)]^{1/2} + 30(\chi_A - \chi_O)^2$$

where D(A-A) and D(O−O) are the single covalent energies of homonuclear bonds and χ_A and χ_O are electronegativities of atom A and oxygen respectively.

The electronegativity values of oxygen, cerium, sodium, lithium and boron are 3.44, 1.12, 0.93, 0.98 and 2.04 respectively [77]. The single bond energy value of Na-Na is 73.08 kJ/ mol, Li-Li 110.21 kJ/mol, Ce-Ce is 245 kJ/mol, B-B is 297 kJ/mol and O−O is 142 kJ/mol [77]. The obtained values of hetero-bond energies are in the following order.

D(B-O) 264.16 kJ/mol < *D*(Na-O) 290.87 kJ/mol < *D*(Li-O) 306.65 kJ/mol< *D*(Ce-O) 347.993 kJ/mol [77]. This revealed that cerium ions make a stable and compact network in lithium glasses as compared to sodium glasses.

The above explanation helps to conclude that the creation of $[BO_4]$ groups and alteration of Ce^{3+} to Ce^{4+} ions are responsible for the shift in the absorption edge in the direction of the higher wavelength that finally leads to a considerable contraction in the band gap.

3.6. Elastic properties

In the light of obtained results of density and band gap energy, here it is very necessary and important to confirm the rigidity of the prepared glasses to correlate all of these outcomes to each other. Elastic property is also one of the essential parameter that is measured for selecting glasses for a specific application. Elastic properties of cerium doped LBC and NaBC glasses are calculated by using Makishima-Mackenzies theory [78-79]. This model is extensively used to compute the elastic parameters based upon the glasses structure and its composition. Different equations used to calculate the elastic constants are mentioned in table 2. The acquired theoretical values of Poisson's ratio (σ), Packing Density (V_T), Young's modulus (E), Bulk modulus (K), Shear modulus (G) and Vickers Hardness (H) of all the glasses are given in Table 5 [78-79].

Packing density and Poisson ratio parameters are directly related with composition and cross link dimensionality of glass network [80]. With the addition of cerium oxide, enhancement of V_T and σ of both glasses increases indicating that coordination of borate groups changes from B3 to B4 groups. This factor is directly related with variation in the cross link density of the glass system.

Glasses are also considered as elastic substances. Any improvement in the value of elastic constants E, K and G can be described on the basis of structural consideration of glass network and its packing density, bond strength and cross linking existence inside the glass system [80]. Presently, the value of these parameters is continuously enhanced as the concentration of modifier oxide (CeO_2) increases. The increased value of young's modulus indicates that the rigidity of glasses increases with the inclusion of CeO_2. The rigid glass structure contains lesser number of oxygens which are non-bridging and are used to change the three fold BO_3 units of boron to four fold BO_4 units [80]. The formation of compact structural units of BO_4 is also responsible for rigidity of glasses [80]. The higher value of the bulk and shear modulus is related

Table 5
Packing Density (V_T), Poisson ratio (σ), Young's Modulus of Elasticity (E), Modulus of Compressibility (K), Modulus of Elasticity in Shear (G) and Vickers Hardness Number (H) of the glass samples.

Glass	Packing Density (V_T)	Poisson ratio (σ)	Young's Modulus of Elasticity (E) (GPa)	Modulus of Compressibility (K) (GPa)	Modulus of Elasticity in Shear (G) (GPa)	Vickers Hardness Number (H) (Kg/mm^2)
NaBC0	0.559	0.252	73.31	49.16	29.29	629.63
NaBC1	0.586	0.263	80.62	56.66	31.92	709.80
NaBC2	0.610	0.272	87.80	64.19	34.51	790.26
NaBC3	0.635	0.281	95.60	72.83	37.31	880.23
NaBC4	0.675	0.294	106.02	85.87	40.96	1007.21
LBC0	0.600	0.268	94.12	67.71	37.11	852.82
LBC1	0.623	0.277	101.25	75.65	39.65	936.30
LBC2	0.648	0.286	108.99	84.73	42.39	1029.51
LBC3	0.703	0.302	122.19	103.06	46.91	1200.05
LBC4	0.751	0.315	134.69	121.32	51.22	1366.91

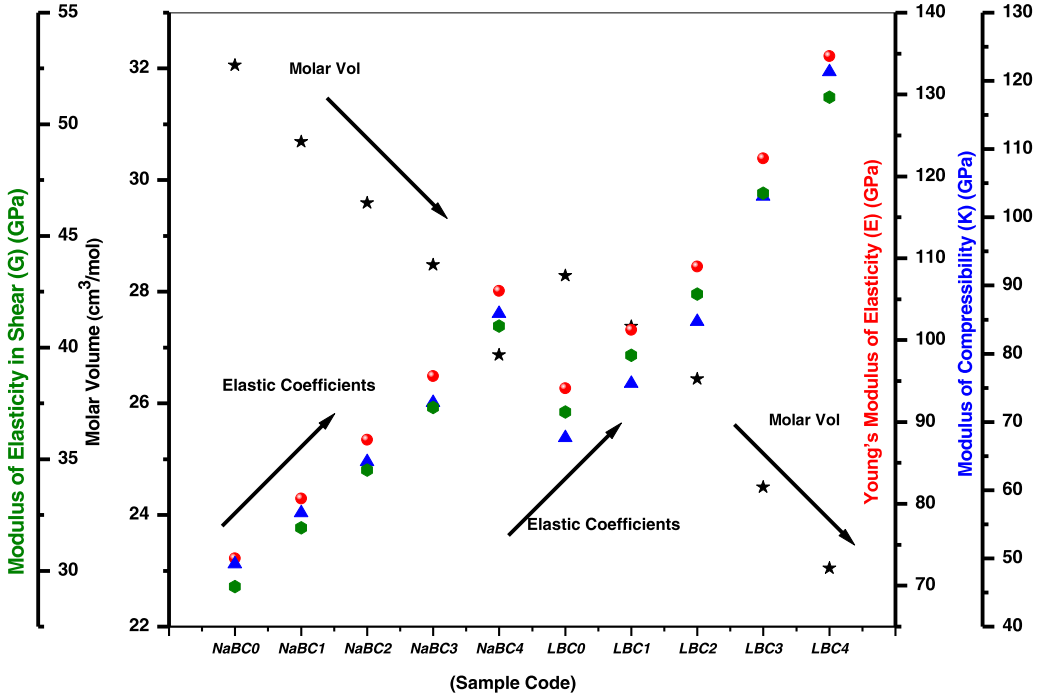

Fig. 9. Variation of E, K and G with Mol% of CeO_2 and Molar volume of glasses.

with the increased value of bond density (n_b) as shown in table 3. The increased value of n_b also helps to increase the elastic modulus. As a result, this also confirms the existence of bridging oxygens. These results favour the continuity in the glasses' structure and hence increase in the rigidity of glasses. The high value of n_b and elastic constants for LBC glasses is an indication of a rigid matrix. For NaBC and LBC glasses, variation of E, K and G with molar volume is represented in Fig. 9.

The Vickers hardness number (VHN) of glass is computed with the help of the equation given by M. Yamane and J.D. Mackenzie [81]. Due to the addition of modifier oxide, VHN of glasses increases with rise in density of glasses. In both glass series, although the hardness number improved with the cerium content yet its value is higher for LBC glasses. This is because the average bond length changes i.e. bond length gets shortened [82]. This can also be elaborated with the result of density/molar volume. Molar volume shrinks as the density of synthesized glasses increases that is because the bond length between modifier cation and oxide decreases [82]. This would help to raise the hardness of glasses. The results i.e. decrease in average boron-boron separation $d_{b\text{-}b}$ and inter nuclear distance (r_i) values also support the increase in VHN as mentioned in table 3. Once more, this validates that the cerium content is altering the glass network. For LBC glasses, VHN has higher value indicating that LBC glasses are more rigid than NaBC glasses.

The higher values obtained for these parameters exposed that both glass series have good mechanical stability. It has been confirmed in prepared glasses that the value of elastic moduli for LBC glasses is more as compared to NaBC glasses. This indicates that cerium oxide plays a more effective role in LBC glass matrix resulting in higher value of stability and rigidity of these glasses. This is again in the support for the existence of tightly packed BO_4 and CeO_4 units in the glass scheme which results in obtaining compact glass structure. The high value of VHN, n_b and elastic constants for LBC glasses is an indication of the rigid glass matrix.

3.7. Photonic view of glasses

To inspect the photonic relevance of the glasses, the TPA (Two-Photon Absorption coefficient) is most appropriate in the area of solid-state photonic devices. It is determined by using the following equation [69].

$$\beta(\mathrm{cm/GW}) = [36.76 - 8.1E_g]$$

where E_g is optical band gap.

The TPA of both the glass series is increasing progressively with the insertion of cerium oxide as presented in Table 4. But for the LBC glasses, TPA has a higher value than NaBC glasses. Here it indicates that LBC glasses may be useful in some photonic devices.

4. Conclusion

The effect of Na_2O and Li_2O content in 70 B_2O_3–(30-x) AO-xCeO_2 glass series has been investigated regarding their physical, structural and optical properties. The addition of alkali metal oxide causes the cleavage of the glass structure thereby disturbing the bonding between glass forming cations and oxygen anions. This results in an escalation in the configuration of more stable tetrahedral [BO_4] constituents as compared to [BO_3] constituents that leads to an extremely compact glass structure formation. This is well depicted in the IR studies as well as in optical studies where, there is a decrease in the optical energy, optical absorption edge alters toward higher frequency, refractive index and optical basicity have shown higher values. Consequently, there is a rise in the OPD (oxygen packing density) and hence enhancement in the density of all the glass samples. The increase in density along with decrease in molar volumes for both the series of these glasses make them more mechanically resistive which is clearly observed as the high values of elastic properties of these glasses such as Poisson's ratio (σ), Packing Density (V_T), Young's modulus (E), Bulk modulus (K), Shear modulus (G) and Vickers Hardness (H) of all the glasses. Another imperative conclusion is that the insertion of cerium oxide in lithium glasses creates more suitable environment that supports the construction of more Ce^{4+} ions. Lastly, TPA has a higher value than NaBC glasses pointing that LBC glasses may be useful in some photonic devices. All the results are more pronounced in case of lithium based glasses which show that the Li-ion concentrations have managed to modify distribution of atoms in the glassy matrix, which affected all of its related structural physical and optical parameters making it more suitable for cerium based glass hosts. Also the refractive index of

lithium glass matrix is on higher side, so could be more suitable for optical fibre glass. The red shift of absorption edge indicates the UV-blocking ability of prepared glasses. This characteristic exposed that in LBC glass series, the controlled value of cerium oxide may be used in some optical filter applications.

CRediT authorship contribution statement

Gurinder Pal Singh: Methodology, Investigation, Resources, Writing - original draft, Validation, Visualization, Software, Investigation, Data curation, Writing - review & editing. **Joga Singh:** Validation, Writing - review & editing. **Parvinder Kaur:** Validation. **Simranpreet Kaur:** Software, Writing - review & editing, Validation. **Deepawali Arora:** Validation. **Ravneet Kaur:** Validation, Writing - review & editing. **D.P. Singh:** Resources, Visualization, Validation, Supervision.

Declaration of Competing Interest

The authors declare that they have no known competing financial interests or personal relationships that could have appeared to influence the work reported in this paper.

References

[1] Y.A. Yamusa, R. Hussin, W.N.W. Shamsuri, Physical, Optical and Radiative properties of $CaSO_4$–B_2O_3–P_2O_5 glasses doped with Sm^{3+} ions, Chin. J. Phys 56 (3) (2018) 932–943.

[2] V.C. Veeranna Gowda, C. Narayana Reddy, K.C. Radha, R.V. Anavekar, J. Etourneau, K.J. Rao, Structural investigations of sodium diborate glasses containing PbO, Bi_2O_3 and TeO_2: elastic property measurements and spectroscopic studies, J, Non-Cryst. Solids 353 (2007) 1150–1163.

[3] N.S. Prabhu, V. Hegde, M.I. Sayyed, E. Şakar, S.D. Kamath, Investigations on the physical, structural, optical and photoluminescence behavior of Er^{3+} ions in Lithium Zinc Fluoroborate glass system, Infrared Phys. Technol. 98 (2019) 7–15.

[4] M.S. Al-Buriahi, A.S. Abouhaswa, H.O. Tekin, C. Sriwunkum, F.I. El-Agawany, T. Nutaro, Y.S. Esra Kavaz, Rammah, Structure, optical, gamma-ray and neutron shielding properties of NiO doped B_2O_3–$BaCO_3$–Li_2O_3 glass systems, Ceram Int 46 (2020) 1711–1721.

[5] N. Ahlawat, S. Sanghi, A. Agarwal, S. Rani, Effect of Li_2O on structure and optical properties of lithium bismosilicate glasses, J. Alloy. Comp. 480 (2009) 516–520.

[6] E. Mansour, FTIR spectra of pseudo-binary sodium borate glasses containing TeO_2, J. Mol. Struct. 1014 (2012) 1–6.

[7] J. Zhong, P.J. Bray, Change in boron coordination in alkali borate glasses and mixed alkali effects, as elucidated by NMR, J. Non-Cryst. Solids 111 (1989) 67–76.

[8] Juliane Steinbrück, Peter W. Nolte, Stefan Schweizer, Far-field studies on Eu3+-doped lithium aluminoborate glass for LED Lighting, not available in VTW/JSS5 (2020), 100046. 10.1016/j.omx.2019.100046.

[9] N.A. Abd El-Malak, Ultrasonic studies on irradiated sodium borate glasses, Mater Chem Phys 73 (2002) 156–161.

[10] Zhiwei Luo, Chunchun Qin, Yanchun Wu, Wenjing Xu, Simin Zhang, Anxian Lu, Structure and properties of Fe2O3-doped 50Li2O-10B2O3-40P2O5 glass and glass-ceramic electrolytes, Solid State Ionics345 (2020), pp. 115177.

[11] Susheela K. Lenkennavar, M.K. Kokila, B. Eraiah, Spectroscopic investigation of different nano metals doped to lead sodium calcium borate glasses, Materials Today: proceedings, in press 10.1016/j.matpr.2020.02.235.2020.

[12] Yasser B. Saddeek, Structural and acoustical studies of lead sodium borate glasses, J. Alloys Compds 467 (2009) 14–21.

[13] Hayder Khudhair Obayesa, Oraskhudhayer Obayes, Qasim Shaker Kadhim, A. Saidu, Mohammed Almaamori, Improved thermoluminescence and kinetic parameters of new strontium/copper co-doped lithium borate glass system, Nuclear Inst. and Methods in Physics Research B 455 (2019) 74–82.

[14] E. Kavaza, H.O. Tekinb, N. Yıldız Yorgund, O.F. Ozdemird, M.I. Sayyed, Structural and nuclear radiation shielding properties of bauxite ore dopedlithium borate glasses: experimental and Monte Carlo study, Rad. Phy. and Chem. 162 (2019) 187–193.

[15] S. A.fyon, F. Krumeich, C. Mensing, A. Borgschulte, R. Nesper, New high capacity cathode materials for rechargeable Li-ion batteries: vanadate-borate glasses, Sci. Rep 4 (2014) 7113.

[16] Amorntep Montreeuppathum, Pinit Kidkhunthod, Saroj Rujirawat, Rattikorn Yimnirun, Supree Pinitsoontorn, Santi Maensiri, Effect of borate glass network to electrochemical properties: manganese doped lithium borate glasses, Rad. Phys. and Chem. 170 (2020) 108677.

[17] Pallati Naresh, Influence of TeO_2 on the UV, electrical and structural studies of Li_2O-ZnO-B_2O_3 glasses, J. Mol. Struct. 1213 (2020) 128184.

[18] A. Madhu, N. Srinath, Structural and spectroscopic studies on the concentration dependent erbium doped lithium bismuth borotellurite glasses for optical fiber applications, Infrared Physics and Technology107 (2020), pp. 103300.

[19] Ke Zhang, Abeer Alaohali, Nuttawan Sawangboon, T Paul, Sharpe,Delia S. Brauer, Eileen Gentleman, A comparison of lithium-substituted phosphate and borate bioactive glasses for mineralised tissue repair, Dental Materials 35 (2019) 919–927.

[20] V.K. Deshpande, Megha A. Salorkar, Nalini Nagpure, Study of lithium ion conducting glasses with Li_2SO_4 addition, J. Non-Cryst. Solids 527 (2020) 119737.

[21] L. Vijayalakshmi, K. Naveen Kumar, Pyung Hwang Dazzling red luminescence dynamics of Eu3+ doped lithium borate glasses for photonic applications, Optik193 (2019), pp. 163019.

[22] E.I. Kamitsos, M.A. Karakassides, Structural studies of binary and pseudo binary sodium borate glasses of high sodium content, Phys. Chem. Glasses 30 (1) (1989) pp.19–pp26..

[23] A.A. Osipov, L.M. Osipova, Structural studies of Na_2O–B_2O_3 glasses and melts using high-temperature Raman spectroscopy, Physica B 405 (2010) 4718–4732.

[24] Lu Deng, Shingo Urata, Yasuyuki Takimoto, Tatsuya Miyajima, Seung Ho Hahn, Adri C.T. van Duin, Jincheng Du, Structural features of sodium silicate glasses from reactive force field-based molecular dynamics simulations, J Am Ceram Soc 103 (2020) 1600–1614.

[25] Hicham Jabraoui, Yann Vaills, Abdellatif Hasnaoui, Michael Badawi, Said Ouaskit, Effect of Sodium Oxide Modifier on Structural and Elastic Properties of Silicate Glass, J. Phys. Chem. B 120 (2016) 51.

[26] A.M. Abdelghany, H.A. ElBatal, F.M. EzzElDin, Bone bonding ability behavior of some ternary borate glasses by immersion in sodium phosphate solution, Ceram. Int 38 (2012) 1105–1113.

[27] E. Ebrahimi, M. Rezvani, Optical and Structural Investigation on Sodium Borosilicate Glasses Doped With CrO, Spectrochimica Acta Part A, Molecular and Biomolecular Spectroscopy 190 (2018) 534–538.

[28] Yasser B. Saddeek, K.A. Aly, A. Dahshan, I.M.El. Kashef, Optical properties of the $Na2O$–B_2O_3–Bi_2O_3–MoO_3 glasses, J Alloys Compd 494 (2010) 210–213.

[29] Juniastel Rajagukguk, Fitrilawati, Bornok Sinaga, Jakrapong Kaewkhao, Structural and spectroscopic properties of Er3+ doped sodium lithium borate glasses, Spectrochimica Acta Part A: Molecular and Biomolecular Spectroscopy 223 (2019) 117342.

[30] J. Rajagukguk, J. Kaewkhao, M. Djamala, M. Hidayat, R. Suprijadi, Y. Ruangtaweep, Structural and optical characteristics of Eu3+ ions in sodium-lead-zinc-lithium-borate glass system, J. mol Struce. 1121 (2016) 180–187.

[31] Hongli Wena, Peter A. Tanner, Optical properties of 3d transition metal ion-doped sodium borosilicate glass, J. Alloys Compd 625 (2015) 328–335.

[32] Priyanka Goyala, Yogesh Kumar Sharma, Sudha Pal, Umesh Chandra Bind, Shu-Chi Huang, Shyan-Lung Chung, Structural, optical and physical analysis of B_2O_3–SiO_2–Na_2O–PbO–ZnO glass with Sm^{3+} ions for reddish–orange laser emission, J Lumin 192 (2017) 1227–1234.

[33] F. Smeacetto, M. Radaelli, M. Salvo, D. Di Modugno, A.G. Sabato, V. Casalegno, M. Broglia, M. Ferraris, Glass-ceramic joining material for sodium-based battery, Ceram. Int. 43 (2017) 8329–8333.

[34] Shams A.M. Issa, Mahmoud Ahmad, H.O. Tekin, Yasser B. Saddeek, M.I. Sayyed, Effect of Bi_2O_3 content on mechanical and nuclear radiation shielding properties of Bi_2O_3-MoO_3-B_2O_3-SiO_2-Na_2O-Fe_2O_3 glass system, Results in Physics 13 (2019) 102165.

[35] A. Aşkın, Evaluation of the radiation shielding capabilities of the Na2B4O7–SiO2–MoO3-Dy2O3 glass quaternary using Geant4 simulation code and Phy-X/PSD database, Ceram Int 46 (2020) 9096–9102.

[36] N.A. Razak, S. Hashim, M.H.A. Mhareb, N. Tamchek, Photoluminescence and thermoluminescence properties of Li2O-Na2O-B2O3 glass31(2016), pp 754–759.

[37] Susheela K. Lenkennavar, M.K. Kokila, B. Eraiah, Spectroscopic investigation of different nano metals doped to lead sodium calcium borate glasses Materials Today: proceedingsin presshttps://doi.org/10.1016/j.matpr.2020.02.235.

[38] Takashi Okada, Yoshiya Taniguchi, Fumihiro Nishimura, Susumu Yonezawa, Solubilization of palladium in molten mixture of sodium borates and sodium carbonate Results in Physics13 (2019), pp 102281.

[39] Pianpian Wu, Xubo Tong, Yang Xu, Jin Han, Xinmin Zhang,Investigation of site occupancy and photoluminescence of Ce in cubic borate BaY(B2O5)3 and Ce3+ → Tb3+ energy transfer behavior, Optical Materials, (2019), pp. 246–252.

[40] R.S. Gedam, D.D. Ramteke, Influence of CeO_2 addition on the electrical and optical properties of lithium borate glasses, J. Phys Chem. Solids 74 (2013) 1399–1402.

[41] Silvia Barbi, Consuelo Mugoni, Monia Montorsi, Mario Affatigato, Corrado Gatto, Cristina Siligardi, Structural and optical properties of cerium oxide doped barium bismuth borate glasses, J. Non-Cryst. Solids 499 (2018) 183–188.

[42] E. Mansour, K. El-Egili, G. El-Damrawi, Ionic–polaronic behavior in CeO_2–PbO–B_2O_3 glasses, Physica B 392 (2007) 221–228.

[43] M.W. Kielty, M. Dettmann, V. Herrig, M.G. Chapman, M.R. Marchewka, A.A. Trofimov, U. Akgun, L.G. Jacobsohn, Investigation of Ce^{3+} luminescence in borate-rich borosilicate glasses, J. Non-Cryst. Solids 471 (2017) 357–361.

[44] Aya Torimoto, Hirokazu Masai, Go Okada, Takayuki Yanagid, Emission properties of cerium-doped barium borate glasses for scintillator applications, Radiat Meas. 106 (2017) 46–51.

[45] K. Annapurna, R.N. Dwivedi, P. Kundu, S. Buddhudu, Blue emission spectrum of Ce^{3+}: znO-B_2O_3-SiO_2 optical glass, Mater. Lett. 58 (2004) 787–789.

[46] Simranpreet Kaur, G Pal Singh, Parvinder Kaur, D.P. Singh, Cerium luminescence in borate glass and effect of aluminium on blue green emission of cerium ions, J. Lumin 143 (2013) 31–37.

[47] U. Caldiño, J.L. H.ernández-Pozos, C. Flores, A. Speghini, M. Bettinelli, Photoluminescence of Ce^{3+} and Mn^{2+} in Zinc metaphosphate glasses, J. Phys. Cond. Mater 17 (2005) 7297–7306.

[48] M. Martini, F. Meinardi, A. Vedda, I. Dafinei, P. Lecoq, M. Nikl, Ce doped hafniate scintillating glasses: thermally stimulated luminescence and photoluminescence, Nucl. Instrum. Methods Phys.Res. B 116 (1996) 116–120.

[49] N. Chiodini, M. Fasoli, M. Martini, E. Rosetta, G. Spinolo, A. Vedda, High-efficiency SiO2:ce^{3+}SiO2:ce^{3+} glass scintillators, Appl. Phys. Lett. 81 (2002) 4374–4376.
[50] Yuki Minami, Jacque Lynn Gabayno, Verdad C. Agulto, Youwei Lai, Melvin John F. Empizo, Toshihiko Shimizu, Kohei Yamanoi, Nobuhiko Sarukura, Akira Yoshikawa, Takahiro Murata, Malgorzata Guzik,Yannick Guyot, Georges Boulon, John A. Harrison, Marilou Cadatal-Raduban, Spectroscopic investigation of praseodymium and cerium co-doped 20Al(PO3)3-80LiF glass for potential scintillator applications, J. Non-Crystl. Solids521(2019), pp. 119495–119542.
[51] Srinivasa Rao Narisimsetti, Megala Rajesh, G.Rajasekhara Reddy, B. Deva Prasad Raju, S. Danapandian, Study of influence of Sm^{3+} ions concentration on fluorescence and FT-IR studies of lead barium lithium borate glasses for red color display device applications, Opt Mater (Amst) 97 (2019) 109360.
[52] Takeo Ejima, Shunsuke Kurosawa, Tadashi Hatano, Toshitaka Wakayama, Takeshi Higashiguchi, Mamoru Kitaura, Luminescence properties of scintillators in soft X-ray region, J Lumin 219 (2020) 116850.
[53] T. Murata, M. Sato, H. Yoshida, K.J. Morinaga, Compositional dependence of ultraviolet fluorescence intensity of Ce^{3+} in silicate, borate, and phosphate glasses, J. Non-Cryst. Solids 351 (2005) 312–316.
[54] E. Varini, S. Sánchez-Salcedo, G. Malavasi, G. Lusvardi, M. Vallet-Regí, A.J. Salinas, Cerium (III) and (IV) containing mesoporous glasses/alginate beads for bone regeneration: bioactivity, biocompatibility and reactive oxygen species activity, Materials Science and Engineering: C 105 (2019) 109971–110028.
[55] Aleksey Starobor, Oleg Palashov, Anastasiia Babkina, Ekaterina Kulpina, Yevgeniy Sgibnev, Yuriy Fedorov, Nikolay Nikonorov, Alexander Ignatiev, Ksenia Zyryanova, Kseniya Oreshkina, Magneto-optical properties of cerium-doped phosphate glass, J Non Cryst Solids 524 (2019) 119644.
[56] M. Karabulut, A. Popa, C. Berghian-Grosan, H. Ertap, M.Yüksek, S. Tokdemir Öztürk, R. Stefan, On the structural features of iron-phosphate glasses by Raman and EPR: observation of superparamagnetic behavior differences in HfO_2 or CeO_2 containing glasses, J. Mole. Struc. 1191 (2019) 59–65.
[57] Marta Sołtys, Agata Górny, Lidia Zur, Maurizio Ferrari, Giancarlo C. Righini, Wojciech A. Pisarski, Joanna Pisarska, White light emission through energy transfer processes in barium gallo-germanate glasses co-doped with Dy^{3+}-Ln^{3+} (Ln =Ce, Tm), Opt Mater (Amst) 87 (2019) 63–69.
[58] S. Yalcin, B. Aktas, D. Yilmaz, Radiation shielding properties of Cerium oxide and Erbium oxide doped obsidian glass, Radiation Physics and Chemistry 160 (2019) 83–88.
[59] Marcin Środa, Szymon Świontek, Wojciech Gieszczyk, Paweł Bilski, The effect of CeO_2 on the thermal stability, structure and thermoluminescence and optically stimulated luminescence properties of barium borate glass, J. Non-Cryst. Solids 517 (2019) 61–69.
[60] G. Pal Singh, Simranpreet Kaur, Parvinder Kaur, D.P. Singh, Modification in structural and optical properties of ZnO,CeO_2 doped Al_2O_3–PbO–B_2O_3 glasses, Physica B 407 (2012) 1250–1255.
[61] G. Pal Singh, D.P. Singh, Spectroscopic study of ZnO doped CeO_2–PbO–B_2O_3 glasses, Physica B 406 (2011) 3402–3405.
[62] J. Krogh-Moe, The structure of vitreous and liquid boron oxide, J. Non-Crystl. Solids 1 (1969) 269–284.
[63] E.I. Kamitsos, M.A. Karakassides, G.D. Chryssikos, Vibrational spectra of magnesium-sodium-borate glasses. 2. Raman and mid-infrared investigation of the network structure, J. Phys. Chem. Glasses 28 (1987) 1073–1079.
[64] E.I. Kamitsos, G.D. Chryssikos, Borate glass structure by Raman and infrared, J. Mole. Struct. 247 (1991) 1–16.
[65] E. Mansour, Structure and electrical conductivity of new Li_2O–CeO_2–B_2O_3 glasses, J. Non-Cryst. Solids 357 (2011) 1364–1369.
[66] A. Ramesh Babua, S. Yusubb, Ascendancy of iron ions on lithium ion conductivity, optical band gap,Urbach energy and topology of LiF-SrO-B_2O_3 glasses, J. Non-Cryst. Solids 533 (2020) 119906.
[67] Vinod Hegdea, C.S. DwarakaViswanathb, Vyasa Upadhyayaa, K.K. Mahatoc, Sudha D. Kamath, Red light emission from europium doped zinc sodium bismuth borate, Physica B 527 (2017) 35–43.
[68] M.A. Marzouk, F.H. ElBatal, H.A. ElBatal, Effect of TiO_2 on the optical, structural and crystallization behavior of barium borate glasses, Opt. Mater. 57 (2016) 14–22.
[69] M. Abdel-Baki, F.A. Abdel-Wahab, Fouad El-Diasty, One-photon band gap engineering of borate glass doped with ZnO for photonics applications, J. Appl. Phys. 111 (2012) 073506.
[70] Kulwinder Kaur, K.J. Singh, Vikas Anand, Correlation of gamma ray shielding and structural properties of PbO–BaO–P_2O_5 glass system, Nuclear Engineering and Design 285 (2015) 31–38.
[71] M.H.A. Mhareba, M.A. Almessierea, M.I. Sayyedd, Y.S.M. Alajerami, Physical, structural, optical and photons attenuation attributes of lithium-magnesium-borate glasses: role of Tm_2O_3 doping, Optik - International Journal for Light and Electron Optics 182 (2019) 821–831.
[72] Nimitha S. Prabhua, Vinod Hegdea, M.I. Sayyed, O. Agarc, Sudha D. Kamatha, Investigations on structural and radiation shielding properties of Er^{3+} doped zinc bismuth borate glasses, Mater Chem Phys 230 (2019) 267–276.
[73] N. Sooraj Hussain, G. Hungerford, R. El-Mallawany, M.J.M. Gomes, M.A. Lopes, Nasar Ali, J.D. Santos, S. Buddhudu, Absorption and Emission Analysis of RE3+(Sm3+ and Dy3+): lithium Boro Tellurite Glasses, J. Nanoscience and Nanotechnology 8 (2008) 1–6.
[74] Kulwinder Kaur, K.J. Singh, Vikas Anand, Structural properties of Bi_2O_3–B_2O_3–SiO_2–Na_2O glasses for gamma ray shielding applications, Radiation Physics and Chemistry 120 (2016) 63–72.
[75] X. Zhao, X. Wang, H. Lin, Z. Wang, A new approach to estimate refractive index, electronic polarizability, and optical basicity of binary oxide glasses Phys, B: Condens. Matter 403 (2008) 2450–2460.
[76] Maria Rita Cicconia, R. Daniel, Neuvilleb Wilfried, Blanc Jean-Francois, Lupic Manuel, Vermillac Dominiquede Lignya, Cerium/aluminum correlation in aluminosilicate glasses and optical silica fiber preforms, J. Non-Cryst. Solids 475 (2017) 85–95.
[77] David R Lide, Handbook of chemistry and physics, 84th edition, CRC press, 2003–2004.
[78] A. Makishima, J.D. Mackenzie, Direct Calculation of Young's Modulus of Glass, J. Non-Cryst. Solids 12 (1973) 35–45.
[79] A. Makishima, J.D. Mackenzie, Calculation of bulk modulus, shear modulus andPoisson's ratio of glass, J. Non-Cryst. Solids 17 (1975) 147–157.
[80] Jingshi Wu, Timothy M. Gross, Liping Huang, Siva Priya Jaccani, Randall E. Youngman, Sylwester J. Rzoska, Michal Bockowski, Saurav Bista, Jonathan F. Stebbins, Morten M. Smedskjaer, Composition and pressure effects on the structure, elastic properties and hardness of aluminoborosilicate glass, J. Non-Cryt. Solids 530 (2020) 119797.
[81] M. Yamane, J. Mackenzie, Vicker's hardness of glass, J. Non-Cryst. Solids 15 (1974) 153–164.
[82] R.A. Tafida, M.K. Halimah, F.D. Muhammad, K.T. Chan, M.Y. Onimisi, A. Usman, A. M. Hamza, S.A. UmarStructural, optical and elastic properties of silver oxide incorporated zinc tellurite glass system doped with Sm3+ ions Materials Chemistry and Physics246 (2020), pp 122801.